



In vivo toxicity assessment of eugenol and vanillin-functionalised silica particles using *Caenorhabditis elegans*

Cristina Fuentes^{a,*}, Samuel Verdú^a, Ana Fuentes^a, María José Ruiz^b, José Manuel Barat^a

^a Department of Food Technology, Universitat Politècnica de València. Camino de Vera s/n, 46022 Valencia, Spain

^b Laboratory of Toxicology, Faculty of Pharmacy, Universitat de València, Av. Vicent Andrés Estellés s/n, Burjassot, 46100 Valencia, Spain

ARTICLE INFO

Edited by Dr. Caterina Faggio

Keywords:

Silicon dioxide
Functionalisation
Nematode
Essential oil components
Oral exposure

ABSTRACT

The toxicological properties of different silica particles functionalised with essential oil components (EOCs) were herein assessed using the *in vivo* model *C. elegans*. In particular, the effects of the acute and long-term exposure to three silica particle types (SAS, MCM-41 micro, MCM-41 nano), either bare or functionalised with eugenol or vanillin, were evaluated on different biological parameters of nematodes. Acute exposure to the different particles did not reduce nematodes survival, brood growth or locomotion, but reproduction was impaired by all the materials, except for vanillin-functionalised MCM-41 nano. Moreover, long-term exposure to particles led to strongly inhibited nematodes growth and reproduction. The eugenol-functionalised particles exhibited higher functionalisation yields and had the strongest effects during acute and long-term exposures. Overall, the vanillin-functionalised particles displayed milder acute toxic effects on reproduction than pristine materials, but severer toxicological responses for the 96-hour exposure assays. Our findings suggest that the EOC type anchored to silica surfaces and functionalisation yield are crucial for determining the toxicological effects of particles on *C. elegans*. The results obtained with this alternative *in vivo* model can help to anticipate potential toxic responses to these new materials for human health and the environment.

1. Introduction

Modification of materials' properties to provide them with novel functionalities gives rise to a wide range of hybrid systems for advanced applications every year (Bagheri et al., 2018; Hildebrand et al., 2006; Lu et al., 2019). Synthetic amorphous silica (SAS) is an ideal candidate for designing hybrid materials due to the high concentration of silanol groups on their surface, large surface area, and good stability and biocompatibility (Bagheri et al., 2018). Different compounds have been used to react with silica surface, which give rise to a wide variety of functional groups, including phenyl, amine, carboxyl or thiol groups, among others (Allothman, 2012). Quite often silica particles have been functionalised with PEG-silanes to enhance particles' biocompatibility and stability (Brown et al., 2007; Hao et al., 2012; He et al., 2011) and with chlorosilanes or alkoxy-silanes as a linker for other functional molecules (Lieberman et al., 2014). Not only small molecules, but also macromolecules like polymers and lipids, can be covalently attached to silica particles' surface (Maleki et al., 2017). One example of these silica-based hybrid structures consists in the functionalisation of silica particles' surface with essential oil components (EOCs) to improve the

antimicrobial activity of these compounds and to reduce their sensory perception in food products (Ribes et al., 2019, 2017; Ruiz-Rico et al., 2018). Despite the efficacy of these antimicrobial devices having been demonstrated, the safety and innocuousness of their use in foods or food contact materials for human health and the environment is still being investigated. Previously, *in vitro* studies have demonstrated that the functionalisation of silica particles with essential oil derivatives prevents their degradation under physiological conditions (Fuentes et al., 2020) and increases the cytotoxic effect on HepG2 cells compared to their free constituents (Fuentes et al., 2021b).

In vitro methods are useful tools for predicting acute toxic effects of chemicals and enhancing our understanding of their mechanisms of action (Eisenbrand et al., 2002). Notwithstanding, when evaluating particles' toxicity after oral exposure, different features like external barriers of the gastro-intestinal tract or their persistence and accumulation in the organism, are not easy to evaluate by *in vitro* assays, and *in vivo* studies are still needed (Gamboa and Leong, 2013; Riediker et al., 2019). Public concerns about using animal models in biological research have led scientists to search for alternatives during the toxicological evaluation of chemicals. One of these alternatives consists in replacing

* Corresponding author.

E-mail address: crifuelp@upvnet.upv.es (C. Fuentes).

vertebrate animals by the non-mammalian model *Caenorhabditis elegans*. This 1 mm-long non-parasitic nematode has become one of the most widely used model organisms in several research fields thanks to its many advantages, such as small size, transparent body, simple anatomy, high reproduction rate, short life cycle and fully-annotated genome (Hunt, 2017; Wu et al., 2019). In addition, many physiological processes are conserved between nematodes and mammals given the presence of homologous genes and proteins (Kaletta and Hengartner, 2006; Leung et al., 2008). Indeed *C. elegans* and human alimentary systems bear many similarities. As in mammals, nematode feeding involves food ingestion, digestion, nutrient absorption and defecation (Gonzalez-Moragas et al., 2017). Moreover, important features like acidified lumen, microvilli, digestive enzymes secretion, uptake of digested components or peristalsis are also found (Hunt, 2017). All these properties make *C. elegans* an excellent *in vivo* model for assessing chemicals' toxicity after oral exposure.

This study aimed to investigate the toxicological properties of different silica particles functionalised with EOCs using the *in vivo* model system *C. elegans*. In particular, the acute and prolonged exposure to three silica particle types (commercial amorphous silica microparticles, mesoporous MCM-41 microparticles and MCM-41 nanoparticles), bare or functionalised with eugenol or vanillin, was evaluated in different biological nematode parameters, such as survival, reproduction, locomotion behaviour or growth. The results obtained with this alternative *in vivo* model will anticipate potential toxicological effects of exposure to these new materials for human health and the environment.

2. Materials and methods

2.1. Reagents and media composition

NGM agar medium and M9 buffer were prepared in the laboratory as described by Stiernagle (2006). NGM agar medium composition was 3 g/L NaCl, 2.5 g/L peptone, 17 g/L agar, 1 M potassium phosphate buffer (108.3 g/L KH_2PO_4 and 35.6 g/L), 1 M CaCl_2 , 1 M MgSO_4 , and 1 mL of 5% cholesterol in ethanol. M9 buffer consisted of 3 g/L KH_2PO_4 , 6 g/L Na_2HPO_4 , 5 g/L NaCl, 1 mL 1 M MgSO_4 .

Synthetic amorphous silica (SAS) microparticles (SYLYSIA® SY350/FCP; 4 (0.1) μm) were supplied by Silysiamont (Italy). N-cetyltrimethylammonium bromide (CTAB), tetraethylorthosilicate (TEOS), chloroform, n-butanone, (3-Aminopropyl) triethoxysilane (APTES), isopropyl alcohol (IPA), formic acid, agar-agar, NaCl, MgSO_4 , and all the other inorganic salts used to prepare *C. elegans* media, were purchased from Scharlab (Spain). Eugenol ($\geq 98\%$ w/w), vanillin ($\geq 98\%$ w/w), KOH, H_2SO_4 , trimethyl orthoformate, Rose Bengal dye (95%) and sodium azide (NaN_3) were provided by Sigma-Aldrich (Spain). Cholesterol (95%) was obtained from Acros Organics (Spain).

2.2. *C. elegans* maintenance and synchronisation

Wild-type *C. elegans* Bristol strain N2 and *Escherichia coli* strain OP50 used in this study were kindly provided by the *Caenorhabditis* Genetics Center (CGC) (University of Minnesota, MN, USA). Worms were maintained on nematode growth media (NGM) agar plates at 20 °C in the dark with an *E. coli* lawn as the food source (Brenner, 1974). Regular sub-culturing by the chunking method was carried out to maintain the *C. elegans* population.

Before the experiments, nematodes were synchronised to obtain uniformly aged populations and to reduce variation. Synchronisation was performed by bleaching gravid hermaphrodite nematodes with an alkaline hypochlorite solution (1 M NaOH, 3% NaClO), followed by washes with M9 buffer. For the acute toxicity tests, eggs were maintained in falcon tubes without food at 20 °C until hatching. Then larvae were transferred to NGM plates with *E. coli* and maintained for 3 days until reaching L4 to the young adult stage. For the long-term toxicity assays, eggs were directly transferred to NMG plates without food and

incubated at 20 °C for a maximum of 16 h to obtain a L1 larvae population.

For all the experiments, *E. coli* suspensions were prepared in M9 buffer with 0.02% v/v cholesterol at a turbidity of 1000 FAU (Formazine Attenuation Units) in a spectrophotometer (ThermoFisher Scientific, Helios Zeta UV-VIS) at 600 nm.

2.3. Preparing materials

Three different silica particle types were used in this study: commercial non-porous amorphous silica microparticles (SAS), MCM-41 microparticles and MCM-41 nanoparticles. Mesoporous silica particles (MCM-41 micro and MCM-41 nano) were synthesised under basic conditions using CTAB as the structure-directing agent and TEOS as the silica precursor. The synthesis process followed for both MCM-41 particle types is fully described by Fuentes et al. (2020).

2.3.1. Functionalisation of silica particles with eugenol

The functionalisation process with eugenol was done by a 3-stage reaction. In a first stage, eugenol aldehyde synthesis was carried out by a Reimer-Tiemann reaction. In this method, 22 mmol of eugenol were dissolved in 150 mL of distilled water at 80 °C in a round-bottomed flask. After cooling to 60 °C, 400 mmol KOH were slowly mixed and then 88 mmol of chloroform were gradually added (1 mL/h for 7 h). The reaction was left to shake at 60 °C overnight, cooled again and acidified with 50 mL of 10% H_2SO_4 (v/v) to reach pH 3. Then purification of the eugenol derivative was performed by extraction with n-butanone and subsequent rotary evaporation. In a second stage, the synthesis of the eugenol alkoxy silane derivative was performed to allow its covalent anchoring to silica particles' surface. In this reaction, eugenol aldehyde was dissolved in 20 mL of IPA, mixed with APTES at a molar ratio of 1:1 (v/v) (4.64 mL) and stirred under reflux at 60 °C for 1 h. In a last stage, the obtained eugenol alkoxy silane derivative was dissolved in 150 mL of IPA and the mixture was divided into three flasks, where 1 g of SAS, 1 g of MCM-41 micro or 0.5 g of MCM-41 nano was added to each one. After 3 h of stirring at room temperature, samples were centrifuged (9000 rpm, 8 min) and submitted to consecutive washing and centrifugation cycles with IPA and distilled water. Finally, the functionalised particles were dried in a vacuum at room temperature for 12 h.

2.3.2. Functionalisation of silica particles with vanillin

The functionalisation process was as follows: 1 g of each silica particle type was mixed with 5 mL of IPA and 362.5 μL of APTES. After stirring for 1 h at room temperature, the mixture was centrifuged (9000 rpm, 8 min) and the supernatant was discarded. Then 250 mg of vanillin previously dissolved in 2.5 mL IPA were added to the precipitate and the mixture was stirred for 1 h. After adding 352.5 μL of trimethyl orthoformate and 120 μL of formic acid, samples were still stirred at 60 °C for 1 h. After cooling, the final particles were washed with IPA and distilled water several times and finally dried in a vacuum at room temperature overnight.

2.4. Materials characterisation

The characterisation of the bare and functionalised particles was performed by instrumental techniques. Transmission electron microscopy (TEM) images were acquired under a Philips CM10 microscope operating at 100 kV. Particle size distribution was measured with dynamic light scattering (DLS) in a Malvern Mastersizer 2000 (Malvern Instruments, UK). The data analysis was based on the Mie theory using a refractive index of 1.45 and absorption indices of 0.01 and 0.1 for the SAS and MCM-41 particles, respectively. A Zeta potential analysis was performed with a Zetasizer Nano ZS (Malvern Instruments, UK). Zeta potential values were calculated from the particle mobility values by applying the Smoluchowski model. Both size distribution and zeta potential measurements were performed in triplicate. Before the analyses,

samples were dispersed in deionised water and sonicated for 2 min to avoid aggregation. Finally, the elemental analysis of the functionalised silica was performed with a CHNS1100 elemental analyser (CE Instruments, UK) to estimate the content of eugenol and vanillin immobilised on particles.

2.5. Particles uptake

Silica particles uptake by *C. elegans* was examined by light microscopy. The bare and functionalised silica particles were stained with crystal violet dye. Then worms were exposed to 1 mg/mL of stained particles in the presence of *E. coli* for 24 h, immobilised with 0.25 M of sodium azide and sealed with coverslips. Nematodes were visualised under a microscope BA310E (Motic, Hong Kong) at 4X magnification and images were captured by a CMOS camera Moticom 3+ (Motic, Hong Kong).

2.6. Toxicity assessment using *C. elegans*

The effects of *C. elegans* exposure to bare and functionalised silica were evaluated using different biological parameters after acute and long-term exposures. A Nine particle types were evaluated: three silica types (SAS, MCM-41 micro, MCM-41 nano), bare or functionalised with two EOCs (eugenol, vanillin). Stock solutions (10 mg/mL) were prepared on M9 buffer and dispersed by sonication in an ultrasound bath for 5 min before each experiment to reduce the formation of agglomerates. Three different concentrations of particles were assayed: 0.2, 1, 5 mg/mL. Negative (M9 buffer) and positive (15 mg/L BAC-C16) controls were included in each plate. All the experiments were carried out in at least three independent weeks. The data obtained from the toxicological assays were expressed as means (SEM).

2.6.1. Acute exposure

Acute toxicity was evaluated on *C. elegans* lethality, reproduction and locomotion behaviour.

Lethality tests were carried out on 24-well culture plates in a final volume of 1 mL of test solution. At least 30 synchronised 3-day-old young adult worms (L4) were transferred to each well. Then plates were incubated at 20 °C in the dark for 24 h. At the end of the exposure time, the numbers of live and dead nematodes were counted. The worms that did not respond to gentle prodding when touched with a platinum wire were scored as dead. The survival rate was calculated as the percentage of live nematodes from the total number of worms per well.

In order to investigate whether acute exposure to particles affected *C. elegans* reproduction, pre-exposed nematodes were individually transferred to 24-well NGM agar plates seeded with *E. coli*. Plates were incubated at 20 °C for 72 h. Then brood size was calculated by counting the number of larvae and eggs laid per adult worm at each time point. Additionally, brood growth was determined by measuring the body length of flat larvae and the surface area of eggs using the Fiji image processing software (Schindelin et al., 2012). The number of pixels occupied by individual worms and eggs was transformed into mm² of previous calibration. The average brood size was calculated for each treatment condition and compared to the control group.

Locomotion assays were carried out in the 24-well NGM agar plates used for the reproduction experiments. Locomotion behaviour was estimated by the tracks produced by worms' sinusoidal movement on solid surfaces. Agar surfaces were captured with a CMOS camera Moticom 3+ (Motic, Hong Kong) connected to a BA310E microscope (Motic, Hong Kong) at 10X magnification. Images were transformed and analysed as described by Fuentes et al. (2022b). The results were expressed as the percentage of agar surface covered by the tracks area generated by worm movement (%).

2.6.2. Long-term exposure

The effect of long-term exposure to particles on *C. elegans*

reproduction and growth was evaluated according to ISO 10872:2010 (ISO, 2010), with slight modifications. Briefly, a drop of M9 buffer containing 5–10 synchronised L1 larvae was transferred to each well of 12-well plates. Then 500 µL of *E. coli* suspension and 500 µL of particles' suspension or M9 buffer (negative control) or 15 mg/L of BAC-C16 (positive control) were added. The positive control BAC-C16 was used for routine analysis to assess performance at each experiment. Plates were incubated at 20 °C in the dark for 96 h. After this time, nematodes were heated at 80 °C for 10 min in an oven and stained with 250 µL of Rose Bengal (0.3 g/L) to kill and straighten nematodes. According to the ISO standard specifications, reproduction and growth were used as toxicity endpoints. Reproduction, as assessed by the fertility rate, was calculated by counting the total number of larvae per well at the end of the test, divided by the total parents included per well. Growth was evaluated by body length by comparing the adult nematode length at the end of experiments to the initial body length of the L1 worms (n = 30) not used in tests. Adult worms were differentiated from the offspring by their size under the microscope. Nematode length was measured by an image analysis as described for the acute exposure assays. Growth inhibition (GI) and reproduction inhibition (RI) were calculated by comparing the exposed worms to the control ones.

2.7. Statistical analysis

The Student's t-test for paired samples was carried out with Statgraphics Centurion XVI (Statpoint Technologies, Inc., USA) to compare the nematodes exposed to test solutions with the control at the different biological endpoints. Statistical significance was considered for $p \leq 0.05$. The multivariate statistical methods of principal component analysis (PCA) and correlation matrix were performed to relate particles' physico-chemical parameters to their toxicological effects on worms using the MATLAB® PLS Tool-box, 6.3 (Eigenvector Research Inc., USA). Only the toxicity endpoints for which significant differences were found between the control and exposed worms according to the Student's t-test were included in the multivariate analysis.

3. Results

3.1. Materials characterisation

A morphological analysis of the bare and functionalised particles was carried out by TEM. Different silica materials types depicted distinct particles' shapes; globular for SAS, angular and elongated for MCM-41 micro and spherical for MCM-41 nano (Fig. 1). Moreover, the TEM images showed the surface pattern of the hexagonal channels characteristic of the inner structure of mesoporous materials in both the bare and functionalised particles. This observation revealed the ordered mesoporous structure of the synthesised MCM-41 materials and the preservation of the structure in the functionalised particles.

Table 1 shows the particle size, the average hydrodynamic diameter and the zeta potential values of the different bare and functionalised materials. The TEM analysis revealed no significant differences in particle size for the different particles both before and after the functionalisation process with both EOCs. However, when particles were characterised by DLS to determine the particle size distribution in aqueous suspensions, SAS particles and MCM-41 nano had considerably higher hydrodynamic particle size values than those obtained by TEM. This effect was particularly relevant for the bare and vanillin-functionalised MCM-41 nano, which increased the mean particle size from 70 nm (as measured by TEM) to a hydrodynamic particle size of 4.34 (0.01) and 3.55 (0.02) µm, respectively. The bare silica particles exhibited negative zeta potential values due to the presence of silanol groups on their surface. After functionalisation, a modification in the zeta potential to positive values was observed independently of the type of silica material and EOC as a result of the presence of alkoxysilane derivatives of the vanillin and eugenol anchored to particles' surfaces.

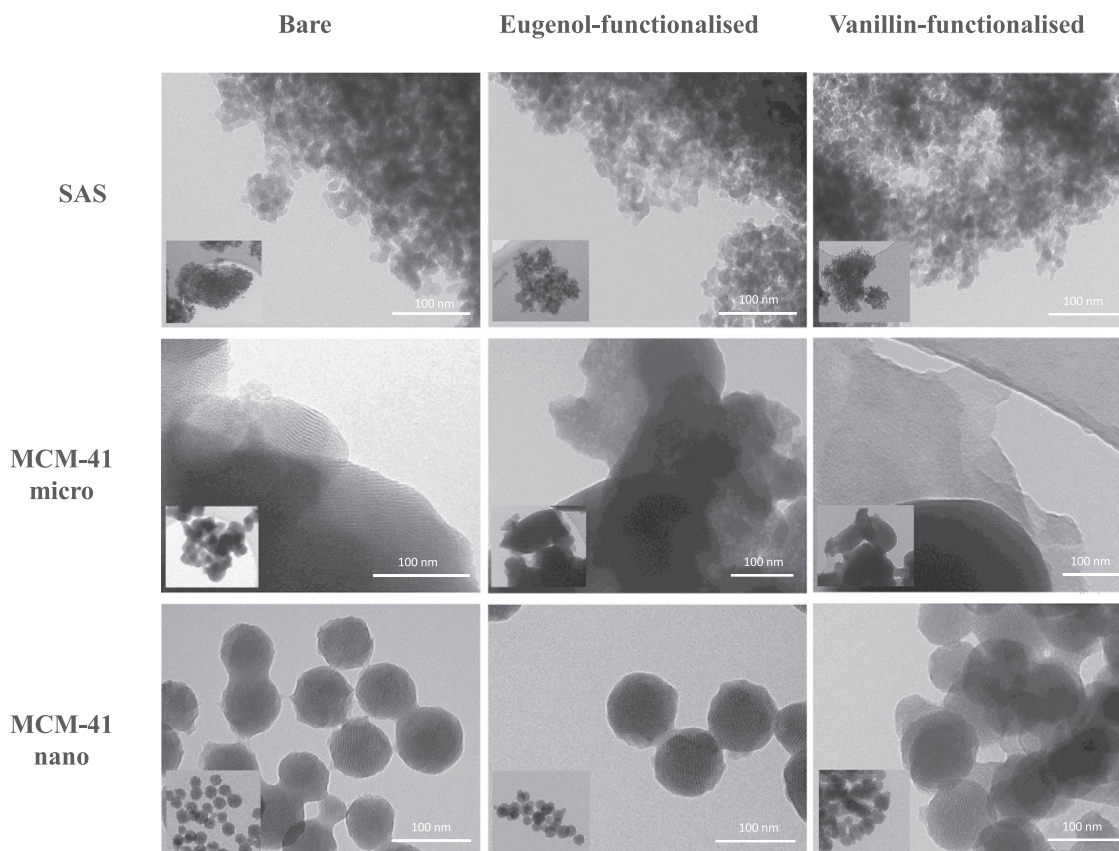


Fig. 1. TEM images of the bare, eugenol- and vanillin-functionalised SAS, MCM-41 micro and MCM-41 nano.

Table 1

Size, particle size distribution ($d_{0.5}$) zeta potential (ZP) and EOC content (α) of the different bare and functionalised silica particle types. Values are expressed as mean (SD, $n = 3$).

Material	Immobilisation	Size (μm)	$d_{0.5}$ (μm) ^a	ZP (mV) ^a	α (g _{EOC} /g _{SiO₂})
SAS	bare	2.49 (0.47)	3.34 (0.02)	-20.93 (0.99)	–
	eugenol	2.03 (0.32)	2.92 (0.01)	11.01 (1.55)	0.0010
	vanillin	2.35 (0.15)	3.37 (0.00)	13.74 (0.65)	0.0307
MCM-41 micro	bare	0.57 (0.09)	0.58 (0.00)	-27.63 (0.71)	–
	eugenol	0.56 (0.13)	0.54 (0.00)	0.19 (1.70)	0.0589
	vanillin	0.63 (0.23)	0.59 (0.00)	17.88 (0.58)	0.0255
MCM-41 nano	bare	0.07 (0.01)	4.34 (0.01)	-31.03 (0.85)	–
	eugenol	0.07 (0.01)	0.58 (0.00)	9.65 (0.73)	0.0860
	vanillin	0.07 (0.01)	3.55 (0.02)	13.47 (0.53)	0.0099

^a Particles dispersed in deionised water.

Finally, the analysis of the elemental composition of the different functionalised materials showed that the highest functionalisation yield was for the MCM-41 micro and the MCM-41 nano functionalised with eugenol, while the worst immobilisation performance was achieved by the eugenol-functionalised SAS particles.

3.2. Particles' uptake

In order to confirm that silica particles were ingested by nematodes, and *C. elegans* could be employed to evaluate oral exposure to these materials, the uptake and accumulation of the stained bare and functionalised silica were evaluated by light microscopy before performing the toxicity tests. As shown in Fig. 2, particles' staining with crystal violet confirmed their oral uptake by worms. After 24 h of exposure, the different silica particle types were observed along the whole nematode intestinal tract, from the buccal cavity and the pharynx to the posterior intestine region and the rectum (Fig. S1).

3.3. Acute toxicity assessment

3.3.1. Lethality

Exposure to the different bare and EOCs-functionalised silica particles for 24 h did not affect nematode survival. No significant differences ($p < 0.05$) were observed between the survival rates of the control and treated worms at any of the tested concentrations. The average survival rates were around 100%, independently of the tested conditions (Fig. S2).

3.3.2. Reproduction

The effect of particles' exposure on nematode reproductive capacity was evaluated by brood size. No differences in the number of larvae laid per worm were observed between the treated and control nematodes, except for the eugenol-functionalised MCM-41 micro and MCM-41 nano at the two highest tested concentrations (Fig. 3). The eugenol-functionalised MCM-41 micro at the concentrations of 1 mg/mL and 5 mg/mL exposure decreased the number of larvae by 45% and 46%, respectively. The percentage of larvae reduction was 52% and 60% compared to the control worms for 1 mg/mL and 5 mg/mL of the

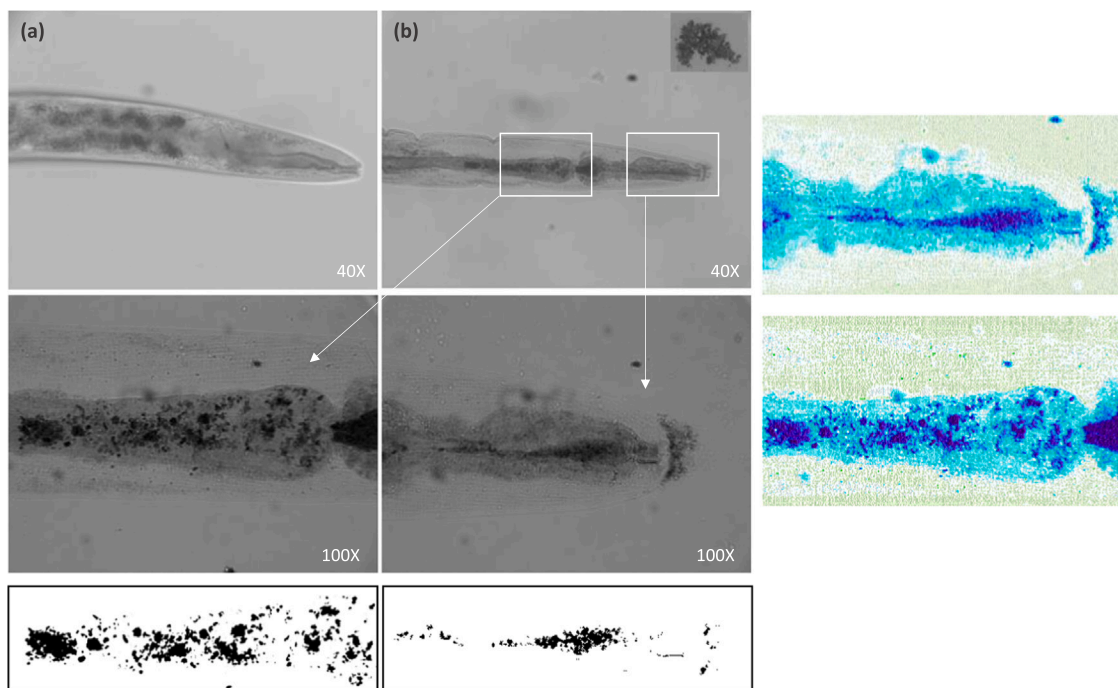


Fig. 2. Representative microscope images (40X magnification) of a control worm (a) and a worm exposed to 1 mg/mL of eugenol-functionalised MCM-41 micro for 24 h (b). Magnification images (100X) of the anterior intestine, the pharynx and the buccal cavity were transformed into black and white (down) and blue tones (right) to improve visualisation.

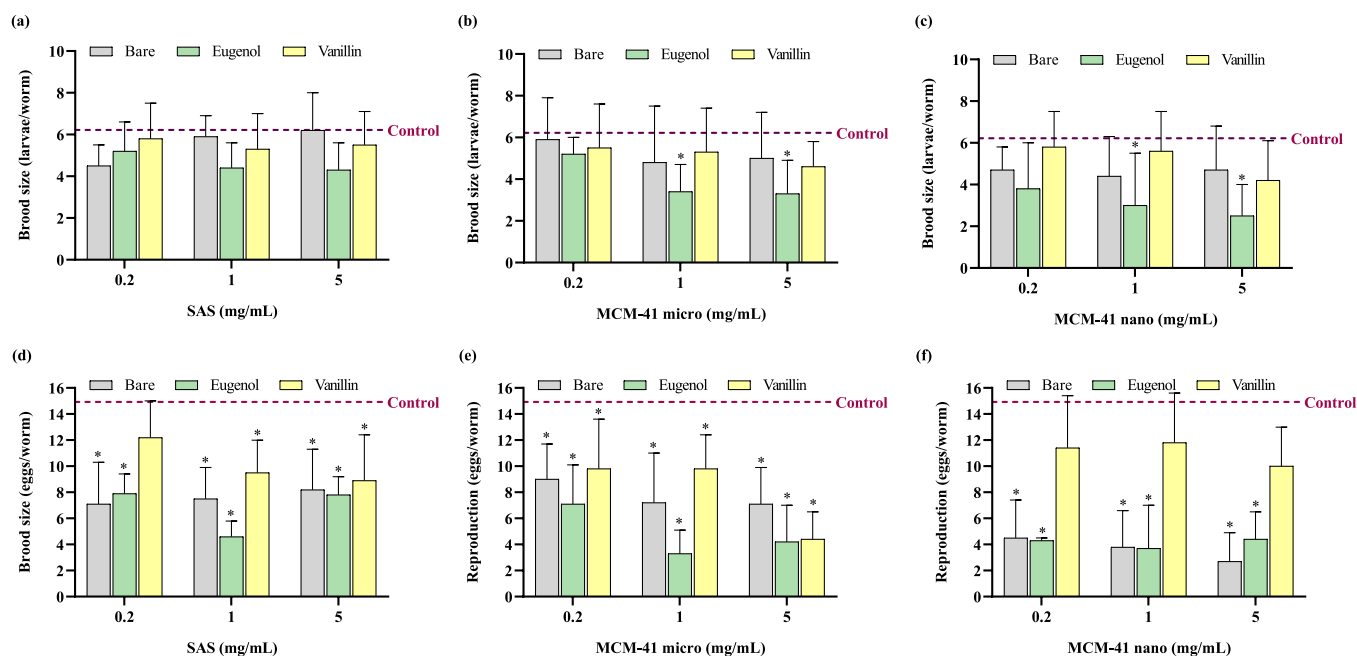


Fig. 3. Effects on *C. elegans* brood size as measured by the larvae born per adult worm after 24 h exposure to the bare, eugenol-functionalised and vanillin-functionalised SAS (a), MCM-41 micro (b) and MCM-41 nano (c). Effects on *C. elegans* brood size as measured by the number of eggs laid per adult worm after 24 h exposure to the bare, eugenol-functionalised and vanillin-functionalised SAS (d), MCM-41 micro (e) and MCM-41 nano (f). Bars express the mean (SEM) of at least three independent assays. (*) $p \leq 0.05$ indicates significant differences compared to the control by the Student's t-test.

eugenol-functionalised MCM-41 nano, and in that order. However, except for vanillin-functionalised MCM-41 nano, the different materials showed an adverse impact on brood size when the number of eggs was used as an endpoint (Fig. 3). The three bare silica particle types reduced egg production, although this effect was more pronounced for MCM-41 nano. Similar results were observed between the bare SAS and bare MCM-41 micro, which reduced brood size by 52% as a maximum in both

cases. The bare MCM-41 nano exposure resulted in stronger effects on reproduction with an 82% decrease in the eggs laid for the 5 mg/mL concentration compared to the control worms (Fig. 3f). Brood size, as measured by egg number, significantly reduced at all the tested concentrations for the eugenol-functionalised materials. This effect was higher for the eugenol-functionalised MCM-41 micro and MCM-41 nano, which showed a maximum respective reduction of 78% and 75% in egg

number at the 1 mg/mL concentration. In contrast, the vanillin-functionalised particles exhibited the mildest effect on nematode reproductive fitness. The vanillin-functionalised SAS reduced egg laying by 40% at the highest tested concentration, while no significant differences were found between 0.2 mg/mL and the control. Vanillin-functionalised MCM-41 micro brought about a 71% reduction for the 5 mg/mL concentration *versus* the control. This value lowered to 34% for both 0.2 and 1 mg/mL of particles. Finally, vanillin-functionalised MCM-41 nano did not significantly affect egg laying at any of the tested concentrations.

Fig. 4 shows brood growth as determined by body larvae length and the surface area of the eggs laid by pre-exposed adults. We can see that none of the bare or functionalised materials affected progeny size at any of the tested concentrations compared to the control group.

3.3.3. Locomotion behavior

The results showed that *C. elegans* did not reduce movement after treatment with any of the different bare and EOCs-functionalised silica particles (Fig. 5). Instead exposure to the bare SAS (0.2 mg/mL), bare MCM-41 micro (5 mg/mL), bare MCM-41 nano (0.2 mg/mL and 1 mg/mL), and also to the vanillin-functionalised SAS (1 mg/mL) and vanillin-functionalised MCM-41 nano (5 mg/mL), resulted in a significant increase in the total area covered by worms.

3.4. Long-term toxicity assessment

Exposure to the different bare and EOCs-functionalised silica particles for 96 h had a significant deleterious effect on both brood size and nematode growth. Inhibition of *C. elegans* reproduction was observed after exposure to all the materials at all the tested concentrations (Fig. 6a–c). A concentration-dependent effect was noted for the bare materials, vanillin functionalised SAS and the different types of studied eugenol-functionalised particles. Exposure to vanillin-functionalised MCM-41 micro and nano resulted in similar reproduction inhibition (RI) percentages. The reduction in brood size ranged from a minimum of 56% for 0.2 mg/mL for the eugenol-functionalised SAS to 100% for 1 mg/mL of the bare MCM-41 micro, bare MCM-41 nano and for all the

different materials at a 5 mg/mL concentration for all three concentrations assayed for vanillin functionalised MCM-41 nano.

Long-term exposure to the bare and EOC-functionalised silica particles caused markedly inhibited nematode growth (Fig. 6d–f). Functionalisation with eugenol led to higher growth inhibition percentages for the three silica particle types at all the tested concentrations, except for 0.2 mg/mL of MCM-41 nano and micro, where vanillin functionalisation caused growth inhibition (GI) to a greater extent. The eugenol-functionalised particles caused 72–95% reductions in body length for SAS, 25–83% for MCM-41 micro and 19–95% for MCM-41 nano. These values ranged from 49% to 74% for the vanillin-functionalised SAS, from 48% to 62% for vanillin-functionalised MCM-41 micro and from 27% to 72% for vanillin-functionalised MCM-41 nano. Finally, the bare silica particles inhibited growth of 27–73%, 3–55% and 24–92% for SAS, MCM-41 micro and MCM-41 nano, respectively.

3.5. Correlation between physico-chemical parameters and toxicity data/multivariate analysis

The Pearson analysis aimed to determine the correlation between the physico-chemical characteristics and the toxicity data. As shown in the Pearson correlation matrix (Table S1), a significant positive correlation was observed between concentration and both long-term exposure assays: RI ($r = 0.4655$; $p = 0.0000$) and GI ($r = 0.4642$; $p = 0.0000$). A significant negative correlation was observed between concentration and the number of eggs laid by worms after acute exposure ($r = -0.2131$; $p = 0.0268$), and also between the functionalisation yield and number of larvae ($r = -0.2941$; $p = 0.0020$) or number of eggs ($r = -0.2078$; $p = 0.0309$) counted during acute tests. Moreover, the functionalisation yield positively correlated with growth inhibition ($r = 0.3347$; $p = 0.0004$). Finally, a positive correlation appeared in the acute endpoints, number of larvae and number of eggs ($r = 0.4816$; $p = 0.0000$), and also between long-term endpoints RI and GI ($r = 0.2539$; $p = 0.0080$).

Simultaneously, the PCA analysis was carried out to reduce dimensionality and to visualise samples distribution and the relation with the original variables. The results revealed that 83.2% of variability was

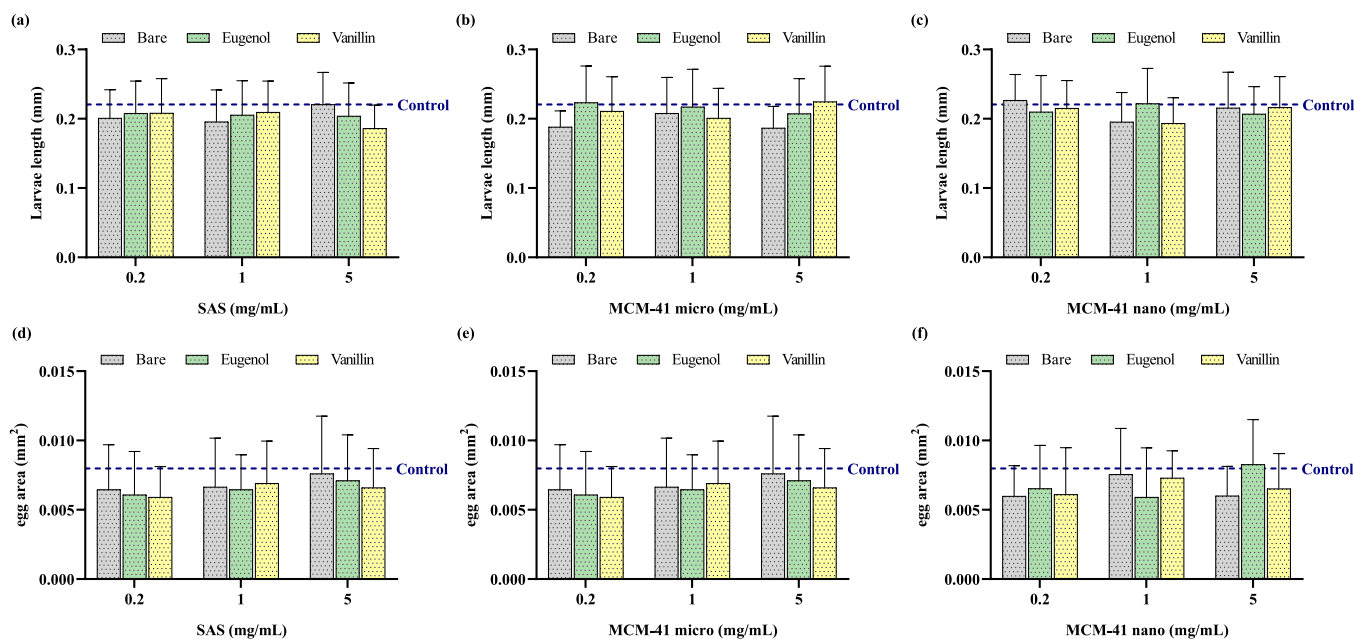


Fig. 4. Effects on *C. elegans* brood growth as measured by the larvae body length from adults after 24 h exposure to the bare, eugenol-functionalised and vanillin-functionalised SAS (a), MCM-41 micro (b) and MCM-41 nano (c). Effects on *C. elegans* brood growth as measured by the eggs laid area per adult worms after 24 h exposure to the bare, eugenol-functionalised and vanillin-functionalised SAS (d), MCM-41 micro (e) and MCM-41 nano (f). Bars express the mean (SEM) of at least three independent assays.

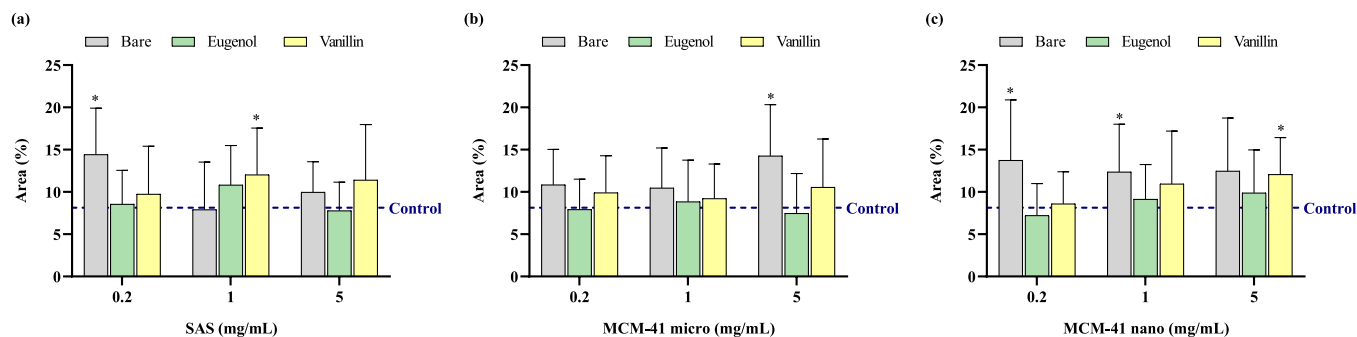


Fig. 5. Area (%) of the tracks generated on the surface of agar wells by the nematodes pre-exposed for 24 h to different concentrations of the bare and EOCs-functionalised SAS (a), MCM-41 micro (b) and MCM-41 nano (c). Bars represent the mean (SEM) of at least three different experiments, and each was carried out in triplicate. (*) $p \leq 0.05$ indicates significant differences compared to the control by the Student's t-test.

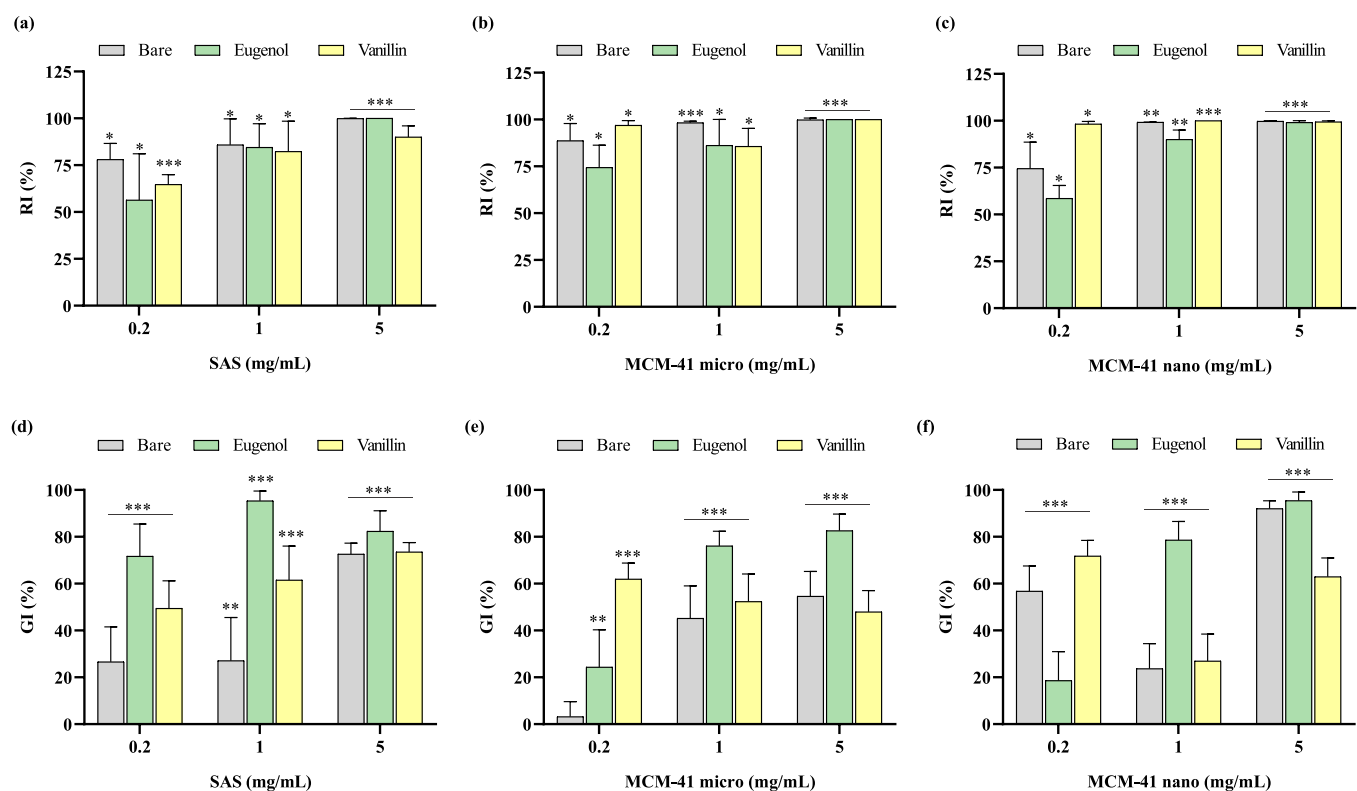


Fig. 6. Inhibition of *C. elegans* reproduction (%) after 96 h exposure to different concentrations of the bare and EOCs-functionalised SAS (a), MCM-41 micro (b) and MCM-41 nano (c). Inhibition of *C. elegans* growth (%) after 96 h exposure to different concentrations of the bare and EOCs-functionalised SAS (d), MCM-41 micro (e) and MCM-41 nano (f). Bars represent the mean (SEM) of at least three different experiments, and each one was carried out in triplicate. (*) $p \leq 0.05$; (**) $p \leq 0.01$; (***) $p \leq 0.001$ indicates significant differences compared to the control by the Student's t-test.

explained by four principal components (Fig. S5). The first principal component (PC1) described 30.5% of total variance, while the second principal component (PC2) described 21.7% (Fig. S5). Together both components explained the largest fraction of the total variance observed for the original variables (52.2%). The most important variables for PC1 were physico-chemical parameters: size distribution and functionalisation yield, and toxicity data: number of larvae, number of eggs and growth inhibition. PC2 was mainly explained by two physico-chemical properties (zeta potential and yield) and three toxicity endpoints (number of larvae and eggs and RI). As shown in Fig. S5, the functionalised-particles were distributed in the upper half of the plot, while the bare materials were clustered in the lower part based on physico-chemical parameters like zeta potential, yield and size distribution. Moreover, the eugenol-functionalised samples were clustered together on the left of the plot according to functionalisation yield, with

low scores for number of larvae and eggs. The vanillin-functionalised and bare particles were clearly separated and located on the right with high progeny production scores.

4. Discussion

Amorphous silica particles have been proposed for a vast number of food, medical and environmental applications. The abundant presence of silanol groups on their surface makes these particles especially favourable for chemical functionalisation, which gives rise to many new materials (Diab et al., 2017). However, their growing production and application increase the risk of exposure for the public and the environment. In this study, the potential toxicity of three types of pristine or EOCs-functionalised amorphous silica particles was evaluated using the *in vivo* model *C. elegans*. This organism has been used to assess different

types of particles' toxicity deriving from oral exposure (Ahn et al., 2014; Angelstorf et al., 2014; Dong et al., 2018; Kim et al., 2020) given the conserved structures and properties from the metabolically active digestive system between nematodes and mammals (Hunt, 2017; Kumar and Suchiang, 2020). Nematode ingestion of particles depends on different *C. elegans* biology factors, such as feeding strategy or buccal cavity size, and also on particle properties like concentration, shape or size (Fueser et al., 2019, 2020a). The light microscopy analysis revealed that all the bare and functionalised particles analysed in this study were ingested by worms during feeding. The different materials were observed in the pharynx and the intestine of nematodes after 24 h of exposure in liquid media, independently of their particle size, agglomeration state or surface functionalisation. In our study, the mean particle size ranged from 70 nm to 2.5 μm , while the average size distribution in aqueous solution ranged from approximately 0.6 μm for the different MCM-41 micro and eugenol-functionalised-MCM-41 nano types to 4.3 μm for the bare MCM-41 nano. According to Fueser et al. (2019), the buccal cavity of nematodes ($4.4 \pm 0.5 \mu\text{m}$) must be at least 1.3-fold larger than the particles to be ingested. Fang-Yen et al. (2009) found that the *C. elegans* pharynx may efficiently transport particles within the size range of most bacterial strains isolated from soil (0.5–3 μm). It has been previously reported that latex microbeads with a maximum diameter of 3.4 μm can be ingested by *C. elegans* (Boyd et al., 2003) or 5.0 μm polystyrene particles are present at low levels in the nematode intestine (Lei et al., 2018), while 6.0 μm polystyrene beads cannot be detected (Fueser et al., 2020b). Having demonstrated that *C. elegans* is an appropriate model system to assess the oral toxicity to these materials, nematodes were exposed to the different silica particles for 24 h and 96 h, and different biological parameters were evaluated, including survival, reproduction, locomotion behaviour or growth.

Acute exposure to the bare and EOCs-functionalised silica particles did not reduce nematode survival, brood growth or locomotion at any of the tested concentrations, but reproduction was impaired as observed by brood size reduction. Smaller brood size may be indicative of delayed egg laying as a consequence of gonad maturation deficiencies or reduced fertility due to a diminished germline in adult hermaphrodites (Williams et al., 2017). However, reproduction inhibition can also be a consequence of effects on other biological processes. Zhang et al. (2020) found fecundity as a more sensitive endpoint than survival, development or behavioural activity when studying exposure to 30 nm amorphous nanosilica for 24 h. According to these authors, the significant reduction in the total number of eggs was a result of a significant increase in apoptotic cell number. Pluskota et al. (2009) observed reduced progeny at increasing concentrations of 50 nm silica nanoparticles, while worms' life span remained unchanged. This effect came with a significant increase in the bag of worms phenotype, an egg laying deficiency characterised by eggs hatching inside the parent's body, which normally occurs in old nematodes. According to these authors, the effect of silica nanoparticles on progeny production was not due to impaired vulva development, but to induced reproductive senescence in nematodes caused by degenerative changes in the reproductive system. Scharf et al. (2013) also found that the reduced egg laying phenotype observed after 24 h of exposure to silica nanoparticles was due to prematurely induced ageing-related phenotypes caused by intracellular nanosilica accumulation in vulval cells. Notwithstanding, Scharf et al. (2016) demonstrated that silica nanoparticles did not modify the morphology or function of vulval muscles, but caused protein aggregation in axons of serotonergic HSN motor neurons to lead to neurotoxicity and ageing pathways. However, all these effects were specific of silica nanoparticles and were not observed when nematodes were exposed to bulk material (500 nm). Given their primary size and their agglomeration state in aqueous suspension, the particles herein studied were not likely to translocate to vulval cells, but to remain in the intestine and cover the vulva's surface of hermaphrodites. So for the herein analysed SAS, MCM-41 micro and MCM-41 nano particles, a more similar scenario to that reported for polystyrene beads exposure would be expected, which

would indirectly inhibit reproduction as a result of heavy body burdens and dietary restrictions caused by these materials (Fueser et al., 2021).

The chronic effects of the different materials' exposure were evaluated according to Standard ISO 10872:2010 (ISO, 2010). The ISO standard specifies a method for determining the toxicity of environmental samples on *C. elegans* growth, fertility and reproduction. Traditionally, this method has been applied to the toxicological evaluation of contaminated water, sediments, soils and waste, but has been more recently and satisfactorily employed for the toxicological assessment of different particle types (Bosch et al., 2018; Hanna et al., 2016). Nematode reproduction and growth were used as endpoints after a 96-hour exposure period to cover the whole nematode development from the four larval stages (L1 to L4) to the hermaphrodite adult stage. Our results showed that all nine particle types significantly reduced both growth and brood size. In general terms for the acute toxicity tests, the eugenol-functionalised particles exhibited the higher inhibition rates. No differences were observed in the reproduction inhibition parameter for the different particle types, and reproductive fitness was a more sensitive parameter after long-term exposure. Furthermore, the correlation between RI and GI could support the notion that hermaphrodite worms did not reach the required body size to be fertile due to particles' exposure and, consequently, reproduction was indirectly inhibited (Schertzingler et al., 2017).

Different physico-chemical properties, such as particle size, shape, surface area and surface chemistry, have been reported to influence their interaction with biological systems and affect the toxic potential of materials *in vitro* and *in vivo* (Heikkilä et al., 2010; Santos et al., 2010; Wu et al., 2019). Therefore, a comprehensive physico-chemical characterisation of the particles under study is crucial during toxicity testing. In this study, the multivariate statistical analysis allowed relations to be established between the physico-chemical parameters of particles and toxicity on *C. elegans*. The results demonstrated that functionalisation, zeta potential and concentration were the most important factors to determine their toxicological effects.

The EOC content in the functionalised particles correlated to reproductive toxicity in the acute assays and to inhibited growth in the long-term exposure experiments. The different eugenol-functionalised silica particles presented high functionalisation yields, high growth inhibition and reduced progeny production after acute exposure, and were more toxic than the vanillin-functionalised or bare silica ones. Of the different silica types used, eugenol-functionalised MCM-41 nano exhibited the highest content of immobilised compound on surfaces and severer toxicological responses. The vanillin-functionalised particles exhibited milder acute toxicity effects, which were similar to or lower than those of the bare particles in some cases. However, greater growth inhibition and lower larvae and eggs production were observed for vanillin-functionalised MCM-41 micro, which also presented a larger amount of immobilised vanillin. Similarly, eugenol had been reported to induce more toxicological effects than vanillin *in vitro* and *in vivo* (Fuentes et al., 2021a). All this information points out that the type and quantity of the EOC anchored to silica surfaces are the most relevant physico-chemical properties to determine their toxic behaviour. These results agree with Verdú et al. (2020), who evaluated the toxicological properties of MCM-41 microparticles that were bare or functionalised with gallic acid. These authors found that the functionalised particles exposure resulted in increased lethality, velocity of movements and a repellent chemotactic effect. These authors attributed the observed toxicological effects to the high local concentrations of immobilised gallic acid on nematode surfaces, which could have toxic effects.

Surface functionality of particles has been demonstrated to determine toxicity by controlling the dispersion state of materials and interactions with *C. elegans* (Jung et al., 2015). Herein the zeta potential values were more positive for the analysed EOCs-functionalised than the bare silica particles. A larger number of electrostatic interactions between positively charged particles and the negative charge of *C. Elegans*' cuticle surface and, consequently a toxic effect, have been suggested

(Wang et al., 2009). However, Que et al. (2020) conducted a comparative toxicological study between bare and amine-functionalised silica nanoparticles on *C. elegans*. They found that exposure to both particle types lowered the survival rate and shortened the life span of nematodes, and reduced progeny production, head thrashing and body bending movements, and significantly shortened body size. However, bare particles were more toxic than amine-functionalised materials as lower doses had a stronger effect on almost all the parameters. The higher toxicity found for the bare silica was attributed by these authors to a disturbance in protein homeostasis caused by a higher interaction between the negatively charged OH groups of its surface and biomolecules, particularly proteins and lipids, compared to the positively charged surface of the amine groups functionalised silica. Similarly, Acosta et al. (2018) reported that starch-functionalisation significantly reduced the toxicity of silica nanoparticles, even if the zeta potential changed from negative to positive upon functionalisation. By taking into account all this information, the nature of the molecules immobilised on particles' surface seems to play a decisive role in toxicity, independently of the electrostatic particle-nematode interactions. In line with this, previous *in vitro* studies demonstrated that carvacrol- and thymol-functionalised MCM-41 microparticles induced toxicity in HepG2 cells by an oxidative stress-related mechanism that resulted in apoptosis through the mitochondrial pathway (Fuentes et al., 2022a). Moreover, oxidative stress has been reported as the main mechanism underlying the cytotoxic behaviour of different EOCs such as eugenol (Fuentes et al., 2021a). As in cells, different essential oils and their main components, including eugenol, have demonstrated antinematodal effects on *C. elegans* (Abdel-Rahman et al., 2013). Lanzerstorfer et al. (2020) found by gene expression analysis, a significant upregulation of xenobiotic and oxidative stress genes, such as superoxide dismutase (sod-3), glutathione S-transferase (gst-4), glutathione peroxidase (gpx-6) and cytochrome P450 family (cyp-14a3), when N2 wild-type and bus-5 mutant nematodes were exposed to low concentrations of rosemary, citrus and eucalyptus essential oils. Additionally, oxidative stress damage has been described as the main mechanism of particles producing toxic effects (Wu et al., 2019). All this information points to an oxidative stress-related mechanism as a possible candidate for the observed increased toxicity of functionalised silica particles in nematodes. However, further investigation using different biological molecular markers is needed for the elucidation of the underlying toxicological mechanism of *C. elegans* to these materials.

An agreement has been reached about considering smaller particles being more toxic than larger particles because of a larger surface area and the better facility to accumulate (Angelstorf et al., 2014; Ma et al., 2019; Wang et al., 2009; Yang et al., 2018). However, some authors have reported that *C. elegans* is more sensitive to particles with a moderate size (Kim et al., 2020; Lei et al., 2018). Lei et al. (2018) found that the lethal effects of microplastic particles exposure on *C. elegans* were independent of chemical composition, but correlated with their size. Of the different analysed particle sizes, the 0.1 μm particles brought about a slight reduction in the survival rate, while the 5.0 μm -sized particles presented moderate lethality. In contrast, the 1 μm particles were the most lethal, caused the most extensive reproductive damage, the lowest level of intestinal calcium and the most accumulation. According to those authors, the toxic effects of microplastics on reproduction and survival are related to the ability to enter and accumulate in nematode intestines, where they induce tissue damage by mechanical injury or insufficient nutrition. In our work, a moderate significant positive correlation was observed between hydrodynamic particle size distribution and the number of larvae laid by worms after acute exposure, while no effect was observed on the other toxicity parameters. However, individual particle size did not affect any analysed toxicity endpoint. Our results support the notion that agglomeration state is more important than primary particle size on the toxicity of the studied materials.

Increasing particle concentrations significantly reduced the number of eggs laid by worms upon acute exposure, which more severely

resulted in increased reproduction and GI after 96 h of exposure. Indeed, during the long-term exposure assay, concentration was the most relevant factor to determine toxicity in nematodes. The likelihood of ingestion of particles at higher concentrations increase as is, therefore, the ability of particles to enter and accumulate in nematodes intestines. As a result, particle accumulation may lead to toxic effects on reproduction and growth. Accordingly, Lei et al. (2018) found a direct relation between intestinal microplastics accumulation and functional damage, as revealed by low calcium levels in exposed *C. elegans*. However, other authors suggest that the particles co-ingested with bacterial cells may reduce food consumption in a particle concentration-dependent manner and result in altered nematode energy-requiring processes, including reproduction (Fueser et al., 2021). Thus, the distribution and accumulation of the particles needs to be addressed in future works by quantitative techniques such inductively coupled plasma mass spectrometry (ICP-MS) to corroborate the accumulation or food deprivation hypothesis.

5. Conclusions

In short, *C. elegans* was employed as an *in vivo* model to determine the toxicological effects deriving from the acute and prolonged exposures to different bare and EOC-functionalised silica particles designed as antimicrobial materials. Particle accumulation was observed in the intestinal tract of the worms exposed to all the different particles under study, which demonstrates the oral ingestion of particles by *C. elegans* during feeding. Reproduction, as measured by brood size, was the most sensitive parameter upon both acute and long-term particle exposures. Acute exposure to the different silica particles neither affected nematode survival or brood growth at any of the tested concentrations nor reduced locomotion behaviour as measured by the tracks area formed by exposed worms. However, reduced brood size was observed after 24 h of exposure to all the different materials, except for vanillin-functionalised MCM-41 nano, and the bare and eugenol-functionalised MCM-41 nano displayed the strongest effects. During the long-term exposure assay, minor differences between the different materials were found in the RI parameter, which almost reached complete reduction in most cases, but eugenol-functionalised resulted in higher GI percentages at higher concentrations. Overall, the eugenol-functionalised particles had the strongest effect on *C. elegans* at both exposure times. The vanillin-functionalised particles had the mildest effect on brood size after 24 h of exposure, while minor differences were observed between the bare and vanillin-functionalised materials upon 96 h of exposure. The analysis of the relation between the physico-chemical parameters of particles and toxicity on *C. elegans* indicated that functionalisation yield, zeta potential and concentration were the most important properties to affect the toxicological effects deriving from particles' exposure. Our findings suggest that the type and quantity of EOC anchored to silica surfaces are crucial for determining the toxicological effects of particles on *C. elegans*, while other properties like particle type or particle size did not seem to play any role. However, these materials' mechanism of action on nematodes still needs to be evaluated. The results obtained with this alternative *in vivo* model can help to anticipate potential toxic responses to new materials for human health and the environment.

CRedit authorship contribution statement

Cristina Fuentes: Conceptualization, Methodology, Investigation, Formal analysis, Data curation, Writing – original draft. **Samuel Verdú:** Methodology, Investigation, Data curation, Formal analysis, Writing – review & editing. **Ana Fuentes:** Conceptualization, Supervision, Writing – review & editing. **María José Ruiz:** Supervision, Writing – review & editing. **José Manuel Barat:** Funding acquisition, Project administration, Supervision.

Declaration of Competing Interest

The authors declare that they have no known competing financial interests or personal relationships that could have appeared to influence the work reported in this paper.

Acknowledgements

The authors are grateful to the Spanish Government (Project RTI2018-101599-B-C21 (MCUI/AEI/FEDER, EU)) and the Generalitat Valenciana (grant agreement no. ACIF/2016/139) for financial support. The authors appreciate the supporting help in providing nematodes from the *Caenorhabditis elegans* Center (CGC), which is funded by the NIH Office of Research Infrastructure Programs (P40 OD010440). Funding for open access charge: Universitat Politècnica de València.

Appendix A. Supporting information

Supplementary data associated with this article can be found in the online version at [doi:10.1016/j.ecoenv.2022.113601](https://doi.org/10.1016/j.ecoenv.2022.113601).

References

- Abdel-Rahman, F.H., Alaniz, N.M., Saleh, M.A., 2013. Nematicidal activity of terpenoids. *J. Environ. Sci. Health Part B* 48, 16–22. <https://doi.org/10.1080/03601234.2012.716686>.
- Acosta, C., Barat, J.M., Martínez-Máñez, R., Sancenón, F., Llopis, S., González, N., Genovés, S., Ramón, D., Martorell, P., 2018. Toxicological assessment of mesoporous silica particles in the nematode *Caenorhabditis elegans*. *Environ. Res.* 166, 61–70. <https://doi.org/10.1016/j.envres.2018.05.018>.
- Ahn, J.M., Eom, H.J., Yang, X., Meyer, J.N., Choi, J., 2014. Comparative toxicity of silver nanoparticles on oxidative stress and DNA damage in the nematode, *Caenorhabditis elegans*. *Chemosphere* 108, 343–352. <https://doi.org/10.1016/j.chemosphere.2014.01.078>.
- Alothman, Z., 2012. A review: fundamental aspects of silicate mesoporous materials. *Materials* 5, 2874–2902. <https://doi.org/10.3390/ma5122874>.
- Angelstorff, J.S., Ahlf, W., von der Kammer, F., Heise, S., 2014. Impact of particle size and light exposure on the effects of TiO₂ nanoparticles on *Caenorhabditis elegans*. *Environ. Toxicol. Chem.* 33, 2288–2296. <https://doi.org/10.1002/etc.2674>.
- Bagheri, E., Ansari, L., Abnous, K., Taghdisi, S.M., Charbgo, F., Ramezani, M., Alibolandi, M., 2018. Silica based hybrid materials for drug delivery and bioimaging. *J. Control. Release*. <https://doi.org/10.1016/j.jconrel.2018.03.014>.
- Bosch, S., Botha, T.L., Jordaan, A., Maboeta, M., Wepener, V., 2018. Sublethal effects of ionic and nanogold on the nematode *Caenorhabditis elegans*. *J. Toxicol.* 2018. <https://doi.org/10.1155/2018/6218193>.
- Boyd, W.A., Cole, R.D., Anderson, G.L., Williams, P.L., 2003. The effects of metals and food availability on the behavior of *Caenorhabditis elegans*. *Environ. Toxicol. Chem.* 22, 3049–3055. <https://doi.org/10.1897/02-565>.
- Brown, S.C., Kamal, M., Nasreen, N., Baumuratov, A., Sharma, P., Antony, V.B., Moudgil, B.M., 2007. Influence of shape, adhesion and simulated lung mechanics on amorphous silica nanoparticle toxicity. *Adv. Powder Technol.* 18, 69–79. <https://doi.org/10.1163/15685520777968214>.
- Diab, R., Canilho, N., Pavel, I.A., Haffner, F.B., Girardon, M., Pasc, A., 2017. Silica-based systems for oral delivery of drugs, macromolecules and cells. *Adv. Colloid Interface Sci.* 249, 346–362. <https://doi.org/10.1016/j.cis.2017.04.005>.
- Dong, S., Qu, M., Rui, Q., Wang, D., 2018. Combinational effect of titanium dioxide nanoparticles and nanopolystyrene particles at environmentally relevant concentrations on nematode *Caenorhabditis elegans*. *Ecotoxicol. Environ. Saf.* 161, 444–450. <https://doi.org/10.1016/j.ecoenv.2018.06.021>.
- Eisenbrand, G., Pool-Zobel, B., Baker, V., Balls, M., Blaauw, B.J., Boobis, A., Carere, A., Kevekordes, S., Lhuguenot, J.C., Pieters, R., Kleiner, J., 2002. Methods of in vitro toxicology. *Food Chem. Toxicol.* [https://doi.org/10.1016/S0278-6915\(01\)00118-1](https://doi.org/10.1016/S0278-6915(01)00118-1).
- Fang-Yen, C., Avery, L., Samuel, A.D.T., 2009. Two size-selective mechanisms specifically trap bacteria-sized food particles in *Caenorhabditis elegans*. *Proc. Natl. Acad. Sci. USA* 106, 20093–20096. <https://doi.org/10.1073/PNAS.0904036106>.
- Fuentes, C., Fuentes, A., Barat, J.M., Ruiz, M.J., 2021a. Relevant essential oil components: a mini-review on increasing applications and potential toxicity. *Toxicol. Mech. Methods* 31, 1–7. <https://doi.org/10.1080/15376516.2021.1940408>.
- Fuentes, C., Fuentes, A., Byrne, H.J., Barat, J.M., Ruiz, M.J., 2022a. In vitro toxicological evaluation of mesoporous silica microparticles functionalised with carvacrol and thymol. *Food Chem. Toxicol.* 160, 112778. <https://doi.org/10.1016/j.fct.2021.112778>.
- Fuentes, C., Ruiz-Rico, M., Fuentes, A., Barat, J.M., Ruiz, M.J., 2021b. Comparative cytotoxic study of silica materials functionalised with essential oil components in HepG2 cells. *Food Chem. Toxicol.* 147, 111858. <https://doi.org/10.1016/j.fct.2020.111858>.
- Fuentes, C., Ruiz-Rico, M., Fuentes, A., Ruiz, M.J., Barat, J.M., 2020. Degradation of silica particles functionalised with essential oil components under simulated physiological conditions. *J. Hazard. Mater.* 399, 123120. <https://doi.org/10.1016/j.jhazmat.2020.123120>.
- Fuentes, C., Verdú, S., Fuentes, A., Ruiz, M.J., Barat, J.M., 2022b. Effects of essential oil components exposure on biological parameters of *Caenorhabditis elegans*. *Food Chem. Toxicol.* 159, 112763. <https://doi.org/10.1016/j.fct.2021.112763>.
- Fueser, H., Mueller, M.T., Traunspurger, W., 2020a. Rapid ingestion and egestion of spherical microplastics by bacteria-feeding nematodes. *Chemosphere* 261, 128162. <https://doi.org/10.1016/j.chemosphere.2020.128162>.
- Fueser, H., Mueller, M.T., Traunspurger, W., 2020b. Ingestion of microplastics by meiobenthic communities in small-scale microcosm experiments. *Sci. Total Environ.* 746, 141276. <https://doi.org/10.1016/j.scitotenv.2020.141276>.
- Fueser, H., Mueller, M.T., Weiss, L., Höss, S., Traunspurger, W., 2019. Ingestion of microplastics by nematodes depends on feeding strategy and buccal cavity size. *Environ. Pollut.* 255, 113227. <https://doi.org/10.1016/j.envpol.2019.113227>.
- Fueser, H., Rauchschaalbe, M.T., Höss, S., Traunspurger, W., 2021. Food bacteria and synthetic microparticles of similar size influence pharyngeal pumping of *Caenorhabditis elegans*. *Aquat. Toxicol.* 235, 105827. <https://doi.org/10.1016/j.aquatox.2021.105827>.
- Gamboa, J.M., Leong, K.W., 2013. In vitro and in vivo models for the study of oral delivery of nanoparticles. *Adv. Drug Deliv. Rev.* <https://doi.org/10.1016/j.addr.2013.01.003>.
- Gonzalez-Moragas, L., Maurer, L.L., Harms, V.M., Meyer, J.N., Laromaine, A., Roig, A., 2017. Materials and toxicological approaches to study metal and metal-oxide nanoparticles in the model organism: *Caenorhabditis elegans*. *Mater. Horiz.* <https://doi.org/10.1039/c7mh00166e>.
- Hanna, S.K., Cooksey, G.A., Dong, S., Nelson, B.C., Mao, L., Elliott, J.T., Petersen, E.J., 2016. Feasibility of using a standardized: *Caenorhabditis elegans* toxicity test to assess nanomaterial toxicity. *Environ. Sci. Nano* 3, 1080–1089. <https://doi.org/10.1039/c6en00105j>.
- Hao, N., Li, Linlin, Zhang, Q., Huang, X., Meng, X., Zhang, Y., Chen, D., Tang, F., Li, Laifeng, 2012. The shape effect of PEGylated mesoporous silica nanoparticles on cellular uptake pathway in HeLa cells. *Microporous Mesoporous Mater.* 162, 14–23. <https://doi.org/10.1016/j.micromeso.2012.05.040>.
- He, Q., Zhang, Z., Gao, F., Li, Y., Shi, J., 2011. In vivo biodistribution and urinary excretion of mesoporous silica nanoparticles: effects of particle size and PEGylation. *Small* 7, 271–280. <https://doi.org/10.1002/sml.201001459>.
- Heikkilä, T., Santos, H.A., Kumar, N., Murzin, D.Y., Salonen, J., Laaksonen, T., Peltonen, L., Hirvonen, J., Lehto, V.-P., 2010. Cytotoxicity study of ordered mesoporous silica MCM-41 and SBA-15 microparticles on Caco-2 cells. *Eur. J. Pharm. Biopharm.* 74, 483–494. <https://doi.org/10.1016/j.ejpb.2009.12.006>.
- Hildebrand, H.F., Blanchemain, N., Mayer, G., Chai, F., Lefebvre, M., Boschin, F., 2006. Surface coatings for biological activation and functionalization of medical devices. *Surf. Coat. Technol.* 200, 6318–6324. <https://doi.org/10.1016/j.surfcoat.2005.11.086>.
- Hunt, P.R., 2017. The C. elegans model in toxicity testing. *J. Appl. Toxicol.* <https://doi.org/10.1002/jat.3357>.
- ISO, 2010. ISO 10872: 2010. Water Quality—Determination of the Toxic Effect of Sediment and Soil Samples on Growth, Fertility and Reproduction of *Caenorhabditis elegans* (Nematoda). Int. Organ. Stand., Geneva, Switzerland, p. 23.
- Jung, S.K., Qu, X., Aleman-Meza, B., Wang, T., Riepe, C., Liu, Z., Li, Q., Zhong, W., 2015. Multi-endpoint, high-throughput study of nanomaterial toxicity in *Caenorhabditis elegans*. *Environ. Sci. Technol.* 49, 2477–2485. <https://doi.org/10.1021/es5056462>.
- Kaletta, T., Hengartner, M.O., 2006. Finding function in novel targets: C. elegans as a model organism. *Nat. Rev. Drug Discov.* <https://doi.org/10.1038/nrd2031>.
- Kim, S.W., Kim, D., Jeong, S.W., An, Y.J., 2020. Size-dependent effects of polystyrene plastic particles on the nematode *Caenorhabditis elegans* as related to soil physicochemical properties. *Environ. Pollut.* 258, 113740. <https://doi.org/10.1016/j.envpol.2019.113740>.
- Kumar, S., Suchiang, K., 2020. *Caenorhabditis elegans*: evaluation of nanoparticle toxicity. In: Model Organisms to Study Biological Activities and Toxicity of Nanoparticles. Springer, Singapore, pp. 333–369. https://doi.org/10.1007/978-981-15-1702-0_17.
- Lanzerstorfer, P., Sandner, G., Pitsch, J., Mascher, B., Aumiller, T., Weghuber, J., 2020. Acute, reproductive, and developmental toxicity of essential oils assessed with alternative in vitro and in vivo systems. *Arch. Toxicol.* 1, 3. <https://doi.org/10.1007/s00204-020-02945-6>.
- Lei, L., Wu, S., Lu, S., Liu, M., Song, Y., Fu, Z., Shi, H., Raley-Susman, K.M., He, D., 2018. Microplastic particles cause intestinal damage and other adverse effects in zebrafish *Danio rerio* and nematode *Caenorhabditis elegans*. *Sci. Total Environ.* 619–620, 1–8. <https://doi.org/10.1016/j.scitotenv.2017.11.103>.
- Leung, M.C.K., Williams, P.L., Benedetto, A., Au, C., Helmcke, K.J., Aschner, M., Meyer, J.N., 2008. *Caenorhabditis elegans*: an emerging model in biomedical and environmental toxicology. *Toxicol. Sci.* 106, 5–28. <https://doi.org/10.1093/toxsci/kfn121>.
- Lieberman, A., Mendez, N., Trogler, W.C., Kummel, A.C., 2014. Synthesis and surface functionalization of silica nanoparticles for nanomedicine. *Surf. Sci. Rep.* <https://doi.org/10.1016/j.surfrep.2014.07.001>.
- Lu, L., Zhu, Z., Hu, X., 2019. Hybrid nanocomposites modified on sensors and biosensors for the analysis of food functionality and safety. *Trends Food Sci. Technol.* <https://doi.org/10.1016/j.tifs.2019.06.009>.
- Ma, H., Lenz, K.A., Gao, X., Li, S., Wallis, L.K., 2019. Comparative toxicity of a food additive TiO₂, a bulk TiO₂, and a nano-sized P25 to a model organism the nematode *C. elegans*. *Environ. Sci. Pollut. Res.* 26, 3556–3568. <https://doi.org/10.1007/s11356-018-3810-4>.
- Maleki, A., Kettiger, H., Schoubben, A., Rosenholm, J.M., Ambrogio, V., Hamidi, M., 2017. Mesoporous silica materials: From physico-chemical properties to enhanced

- dissolution of poorly water-soluble drugs. *J. Control. Release.* <https://doi.org/10.1016/j.jconrel.2017.07.047>.
- Pluskota, A., Horzowski, E., Bossinger, O., von Mikecz, A., 2009. In *Caenorhabditis elegans* nanoparticle-bio-interactions become transparent: silica-nanoparticles induce reproductive senescence. *PLoS One* 4, e6622. <https://doi.org/10.1371/journal.pone.0006622>.
- Que, D.E., Hou, W.-C., Yap Ang, M.B.M., Lin, C.-C., 2020. Toxic effects of hydroxyl- and amine-functionalized silica nanoparticles (SiO₂ and NH₂-SiO₂ NPs) on *Caenorhabditis elegans*. *Aerosol Air Qual. Res.* 20 <https://doi.org/10.4209/aaqr.2020.04.0157>.
- Ribes, S., Ruiz-Rico, M., Pérez-Esteve, É., Fuentes, A., Barat, J.M., 2019. Enhancing the antimicrobial activity of eugenol, carvacrol and vanillin immobilised on silica supports against *Escherichia coli* or *Zygosaccharomyces rouxii* in fruit juices by their binary combinations. *LWT* 113, 108326. <https://doi.org/10.1016/j.lwt.2019.108326>.
- Ribes, S., Ruiz-Rico, M., Pérez-Esteve, É., Fuentes, A., Talens, P., Martínez-Máñez, R., Barat, J.M., 2017. Eugenol and thymol immobilised on mesoporous silica-based material as an innovative antifungal system: application in strawberry jam. *Food Control* 81, 181–188. <https://doi.org/10.1016/j.foodcont.2017.06.006>.
- Riediker, M., Zink, D., Kreyling, W., Oberdörster, G., Elder, A., Graham, U., Lynch, I., Duschl, A., Ichihara, G., Ichihara, S., Kobayashi, T., Hisanaga, N., Umezawa, M., Cheng, T.J., Handy, R., Gulumian, M., Tinkle, S., Cassee, F., 2019. Particle toxicology and health - where are we? Part. *Fibre Toxicol.* <https://doi.org/10.1186/s12989-019-0302-8>.
- Ruiz-Rico, M., Pérez-Esteve, É., de la Torre, C., Jiménez-Belenguer, A.I., Quiles, A., Marcos, M.D., Martínez-Máñez, R., Barat, J.M., 2018. Improving the antimicrobial power of low-effective antimicrobial molecules through nanotechnology. *J. Food Sci.* 83, 2140–2147. <https://doi.org/10.1111/1750-3841.14211>.
- Santos, H.A., Riikonen, J., Salonen, J., Mäkilä, E., Heikkilä, T., Laaksonen, T., Peltonen, L., Lehto, V.-P., Hirvonen, J., 2010. In vitro cytotoxicity of porous silicon microparticles: effect of the particle concentration, surface chemistry and size. *Acta Biomater.* 6, 2721–2731. <https://doi.org/10.1016/j.actbio.2009.12.043>.
- Scharf, A., Gührs, K.H., Von Mikecz, A., 2016. Anti-amyloid compounds protect from silica nanoparticle-induced neurotoxicity in the nematode *C. elegans*. *Nanotoxicology* 10, 426–435. <https://doi.org/10.3109/17435390.2015.1073399>.
- Scharf, A., Piechulek, A., Von Mikecz, A., 2013. Effect of nanoparticles on the biochemical and behavioral aging phenotype of the nematode *Caenorhabditis elegans*. *ACS Nano* 7, 10695–10703. <https://doi.org/10.1021/nn403443r>.
- Schertzinger, G., Zimmermann, S., Grabner, D., Sures, B., 2017. Assessment of sublethal endpoints after chronic exposure of the nematode *Caenorhabditis elegans* to palladium, platinum and rhodium. *Environ. Pollut.* 230, 31–39. <https://doi.org/10.1016/j.envpol.2017.06.040>.
- Schindelin, J., Arganda-Carreras, I., Frise, E., Kaynig, V., Longair, M., Pietzsch, T., Preibisch, S., Rueden, C., Saalfeld, S., Schmid, B., Tinevez, J.Y., White, D.J., Hartenstein, V., Eliceiri, K., Tomancak, P., Cardona, A., 2012. Fiji: an open-source platform for biological-image analysis. *Nat. Methods* 9, 676–682. <https://doi.org/10.1038/nmeth.2019>.
- Stiernagle, T., 2006. Maintenance of *C. elegans*. *WormBook.* <https://doi.org/10.1895/wormbook.1.101.1>.
- Verdú, S., Ruiz-Rico, M., Perez, A.J., Barat, J.M., Talens, P., Grau, R., 2020. Toxicological implications of amplifying the antibacterial activity of gallic acid by immobilisation on silica particles: a study on *C. elegans*. *Environ. Toxicol. Pharmacol.* 80, 103492. <https://doi.org/10.1016/j.etap.2020.103492>.
- Wang, H., Wick, R.L., Xing, B., 2009. Toxicity of nanoparticulate and bulk ZnO, Al₂O₃ and TiO₂ to the nematode *Caenorhabditis elegans*. *Environ. Pollut.* 157, 1171–1177. <https://doi.org/10.1016/j.envpol.2008.11.004>.
- Williams, D.C., Bailey, D.C., Fitsanakis, V.A., 2017. *Caenorhabditis elegans* as a model to assess reproductive and developmental Toxicity. *Reprod. Dev. Toxicol.* 303–314. <https://doi.org/10.1016/B978-0-12-804239-7.00017-2>.
- Wu, T., Xu, H., Liang, X., Tang, M., 2019. *Caenorhabditis elegans* as a complete model organism for biosafety assessments of nanoparticles. *Chemosphere* 221, 708–726. <https://doi.org/10.1016/j.chemosphere.2019.01.021>.
- Yang, Y., Xu, G., Xu, S., Chen, S., Xu, A., Wu, L., 2018. Effect of ionic strength on bioaccumulation and toxicity of silver nanoparticles in *Caenorhabditis elegans*. *Ecotoxicol. Environ. Saf.* 165, 291–298. <https://doi.org/10.1016/j.ecoenv.2018.09.008>.
- Zhang, F., You, X., Zhu, T., Gao, S., Wang, Y., Wang, R., Yu, H., Qian, B., 2020. Silica nanoparticles enhance germ cell apoptosis by inducing reactive oxygen species (ROS) formation in *Caenorhabditis elegans*. *J. Toxicol. Sci.* 45, 117–129. <https://doi.org/10.2131/jts.45.117>.